Struct Chem (2016) 27:1005–1016
DOI 10.1007/s11224-015-0733-2

ORIGINAL RESEARCH

Charge-assisted $N^{(+)}$–$H\cdots^{(-)}S$ hydrogen bonds in the crystal structure of selected diammonium thiophenolates

Katarzyna Kazimierczuk[1]

Received: 10 November 2015 / Accepted: 19 December 2015 / Published online: 8 January 2016

Abstract New salts of thiophenol with three flexible aliphatic diamines $H_2N(CH_2)_nNH_2$ ($n = 2$, 4 and 6) have been synthesized and characterized by elemental analyses, IR spectroscopy and X-ray crystallography in order to analyze their supramolecular architecture. Structural analyses indicate that in the crystals, proton transfer has occurred, with the –SH group giving $^{(+)}N$–$H\cdots S^{(-)}$ hydrogen bonding interaction. The structure of compound **1** exhibits a two-dimensional network and compounds **2–3** a three-dimensional supramolecular networks, and each of them is based on hydrogen bonds and CH···π interactions. The transfer of proton from the thiol to the diamines was confirmed by the solid-state FTIR spectra of **1–3**.

Keywords Hydrogen bonding · Thiolates · Ammonium salts · X-ray structure · FTIR studies

Introduction

Crystal engineering is an interdisciplinary field that combines organic and inorganic chemistry, X-ray crystallography, physical and theoretical chemistry and supramolecular chemistry [1]. Its purpose is an in-depth understanding of the impact of intermolecular interactions on the crystal structure of ordered solid phases. The understanding will allow to fulfill the main purpose of the crystalline engineering, i.e., the rational design of crystals structures [2]. Designed in this way, the crystal will exhibit the pre-defined chemical reactivity or optical, magnetic or mechanical properties. Many types of weak interactions are responsible for packing of molecules in crystals. Apart from well-known non-covalent forces such as dipole–dipole or dipole-transient–dipole interactions, new bonding types are identified. These are, for example, δ-hole interactions—especially halogen bonding [3, 4]. Hydrogen bonding is unquestionably the most important cohesive force in directing the supramolecular organization in the solid state [5]. It is relatively strong, directional and very diverse and widespread. It allows to largely provide for the organization of molecules, at least in two dimensions. Synthon is defined as a part of the molecule under consideration that contains atoms, bonds and stereochemical information needed to obtain the target structure. Synthon is a repeatable pattern within the crystal structure. However, there is usually no simple connection between the crystal structure and the molecular structure, because the behavior of functional group in the molecule during the crystallization depends on the nature and position of all the other function groups [6]. That is why one of the practical purposes of crystal engineering is to describe similar molecules that lead to analogous crystal structures. If particle similarity leads to similar packing in the form of synthons of the same type, the use of molecules with a comparable structure may help in predicting the crystal structure of other compounds.

The hydrogen bond is a very effective design element in crystal engineering [7–9]. A very large variety of hydrogen bonds are known, but hydrogen bonds with sulfur as a donor are not well studied. The –SH group is a weaker donor than, for example, the –OH group (S has smaller electronegativity 2.5 compared to 3.5 for O). Nevertheless, the –SH group may simultaneously act as hydrogen bond donor and acceptor, analogous to –OH [10]. There are

✉ Katarzyna Kazimierczuk
katarzyna.kazimierczuk@pg.gda.pl

[1] Department of Chemistry, Gdańsk University of Technology, G. Narutowicza St. 11/12, 80-233 Gdańsk, Poland

Table 1 Crystallographic data and structure refinement details for compounds **1**–**3**

Compound reference	**1** (CCDC 1430358)	**2** (CCDC 1430359)	**3** (CCDC 1430360)
Empirical formula	$C_7H_{10}NS$	$C_{48}H_{70}N_6S_6$	$C_{18}H_{28}N_2S_2$
M g/mol	140.22	923.46	336.54
Temperature/K	150(2)	120(2)	120(2)
Wavelength/Å	0.71073 (Mo K_α)	0.71073 (Mo K_α)	0.71073 (Mo K_α)
Crystal system	Monoclinic	Monoclinic	Triclinic
Space group	*C*2/c	*P*2/c	*P*−1
a/Å	31.413(6)	17.8014(8)	8.6042(4)
b/Å	6.0882(12)	5.66330(10)	9.5995(4)
c/Å	7.9775(16)	31.1469(11)	12.1506(6)
α/°			110.639(4)
β/°	100.35(3)	124.596(3)	90.189(4)
γ/°			91.630(4)
V/Å^3	1500.9(5)	2584.82(17)	938.71(7)
Z	8	2	2
Calculated density/Mg m^{-3}	1.241	1.186	1.191
F(000)	600	992	364
θ range/°	2.64–25.88	2.639–25.247	2.34–25.5
Limiting indices	−38 ≤h ≤38	−21 ≤h ≤21	−10 ≤h ≤10
	−7 ≤k ≤6	−6 ≤k ≤6	−11 ≤k ≤11
	−9 ≤l ≤9	−33 ≤l ≤37	−14 ≤l ≤14
Reflections collected/unique	4878/1423	16508/4687	5844/3500
	[R(int) = 0.1007]	[R(int) = 0.0156]	[R(int) = 0.0208]
Completeness to θ_{max}/%	97.7	99.9	99.9
Refinement method	Full-matrix least-squares on F^2	Full-matrix least-squares on F^2	Full-matrix least-squares on F^2
Data/restraints/parameters	1423/0/94	4687/0/323	3500/0/223
Goodness of fit on F^2	1.072	1.333	1.078
Final R indices [I > 2sigma(I)]	R1 = 0.0387	R1 = 0.0589	R1 = 0.0409
	wR2 = 0.1154	wR2 = 0.1532	wR2 = 0.1017
R indices (all data)	R1 = 0.0420	R1 = 0.0629	R1 = 0.0505
	wR2 = 0.1187	wR2 = 0.1571	wR2 = 0.1052
Largest diff. peak and hole/eÅ^{-3}	0.305; −0.525	0.867; −0.296	0.564; −0.204

several types of hydrogen bonds in the N···H···S system. The Cambridge Structural Database (CSD) version 5.36 (February 2015 update) [11] was now examined to find out the generality of occurrence of crystal structures which contain N···H···S interactions. Inert systems featuring N–H···S can be found in the thiocarbonyl [12–15] or thioether [16] compounds. Second, electrically neutral N···H–S hydrogen bonds are rarely found in the solid state [17–19], because the SH group is a weak proton donor and forms bonds of low energy. There are several types of hydrogen bonds endowed with electric charge $^{(+)}$N–H···S [20, 21], N–H···S$^{(-)}$ [22, 23], $^{(+)}$N–H···S$^{(-)}$ [24, 25] or less likely $^{(-)}$N···H–S$^{(+)}$ The most interesting case is the charge-assisted $^{(+)}$N–H···S$^{(-)}$ hydrogen bond proton transfer leads to the doubly charged system, and the hydrogen bond is further stabilized by electrostatic attraction between ions.

In recent years, we have described of many structures of ammonium thiolates and silanethiolates featuring the charge-assisted $^{(+)}$N–H···S$^{(-)}$ hydrogen bonds. Application of primary amines leads to tetrameric salts with a core bound by a 'cubane-like' hydrogen bonding net [26]. Secondary amines give derivatives with discrete dimeric units in the solid state [27–29]. So we have finite, 'point type' or zero-dimensional hydrogen bonds that cannot create crystal-wide web in both cases. In order to obtain further insight into these complex intermolecular interactions, research on bifunctional ammines [30] and polyamines [31] was undertaken. The molecular structures and crystal packings are of the studied systems stabilized by intermolecular N–H···S, N–H···N, N–H···O and O–H···S hydrogen bonds into an infinite two-dimensional network.

Table 2 Hydrogen bond parameters in structures **1–3**

D–H···A	d(D–H)/Å	d(H···A)/Å	d(D···A)/Å	∠ (DHA)/°
1				
N(1)–H(1A)···S(1)$^{\#1}$	0.91(3)	2.27(3)	3.169(2)	175(2)
N(1)–H(1B)···S(1)$^{\#2}$	0.83(2)	2.42(2)	3.213(2)	160(2)
N(1)–H(1C)···S(1)	0.85(2)	2.40(2)	3.205(2)	160(2)
C(5)–H(5)···Cg(1)$^{\#3}$	0.95	2.93	3.718(2)	141
2				
N(1)–H(1A)···S(1)$^{\#4}$	0.98(5)	2.20(5)	3.175(3)	173(4)
N(1)–H(1B)···S(2)$^{\#5}$	0.89(4)	2.38(4)	3.262(3)	169(3)
N(1)–H(1C)···S(2)	0.96(5)	2.32(5)	3.275(3)	170(3)
N(2)–H(2A)···S(3)$^{\#5}$	0.84(4)	2.45(5)	3.285(3)	176(4)
N(2)–H(2B)···S(3)	0.87(4)	2.39(5)	3.241(3)	168(4)
N(2)–H(2C)···S(2)	0.97(4)	2.33(4)	3.286(3)	170(3)
N(3)–H(3A)···S(1)	0.92(5)	2.29(5)	3.203(3)	173(3)
N(3)–H(3B)···S(1)$^{\#5}$	0.89(4)	2.33(5)	3.155(3)	155(3)
N(3)–H(3C)···S(3)$^{\#6}$	0.95(4)	2.29(4)	3.235(3)	173(3)
C(4)–H(4)···Cg(2)	0.95	2.67	3.531(5)	150
C(10)–H(10)···Cg(3)$^{\#7}$	0.95	2.61	3.498(4)	157
C(15)–H(15)···Cg(1)$^{\#1}$	0.95	2.72	3.433(4)	132
C(19)–H(19B)···Cg(1)	0.99	2.97	3.825(3)	145
C(22)–H(22A)···Cg(2)	0.99	2.98	3.825(4)	144
3				
N(1)–H(1A)···S(2)$^{\#8}$	0.89(2)	2.38(2)	3.270(2)	171(2)
N(1)–H(1B)···S(1)$^{\#9}$	0.97(3)	2.26(3)	3.221(2)	171(2)
N(1)–H(1C)···S(1)$^{\#10}$	0.90(2)	2.38(3)	3.243(2)	161(2)
N(2)–H(2A)···S(1)	0.92(2)	2.37(2)	3.246(2)	161(2)
N(2)–H(2B)···S(2)$^{\#11}$	0.89(3)	2.35(3)	3.227(2)	169(2)
N(2)–H(2C)···S(2)	0.92(2)	2.35(2)	3.251(2)	166(2)
C(13)–H(13B)···Cg(1)$^{\#12}$	0.99	2.77	3.556(2)	136
C(18)–H(18B)···Cg(2)$^{\#13}$	0.99	2.84	3.538(2)	128

Cg(1), Cg(2) and Cg(3) are the centers of gravity of the C1–C6, C7–C12 and C13–C18 rings, respectively

Symmetry codes: #1: x,−y+1,z−½; #2: x,y−1,z; #3: x,y−2,z−½; #4: −x,y+1,−z+½; #5: x,y+1,z; #6: x,−y+1,z+½; #7: −x+1,y, −z+½;#8: −x+1,−y+1,−z+1; #9: x,y+1,z+1; #10: −x+2,−y+1,−z+1; #11: −x+1,−y+1,−z; #12: −x+1,−y,−z+1; #13: −x,−y+1,−z+1

In this work, we reported the supramolecular patterns of salts assembled by thiophenol with three flexible aliphatic diamines. The main aim of this work was to study how the different lengths of the aliphatic spacers –(CH_2)n–($n = 2$, 4 and 6) will influence the final structures of the salts. From the standpoint of crystal engineering and supramolecular chemistry, the structure of salts mainly depends on the intermolecular non-covalent bonding N–H···S bonding interactions.

Structural analyses indicate that the proton transfer from S–H to N across an S···N bridge is facile as it was in the case of ammonium silanethiolates or thiolates and imidazolium silanethiolates [32].

Experimental section

Materials and measurements

All reagents were obtained from commercial suppliers. The solvents and amines were dried by standard methods and distilled under argon prior to use. All reactions and manipulations were carried in an inert atmosphere of argon employing standard Schlenk vacuum line techniques. Elemental analyses were performed on elemental analyzer Ea 1108 (Carlo Erba Instruments). The FTIR spectra were measured for crystalline compounds in the range of 4000–400 cm^{-1} with a Nicolet iS50 spectrometer equipped

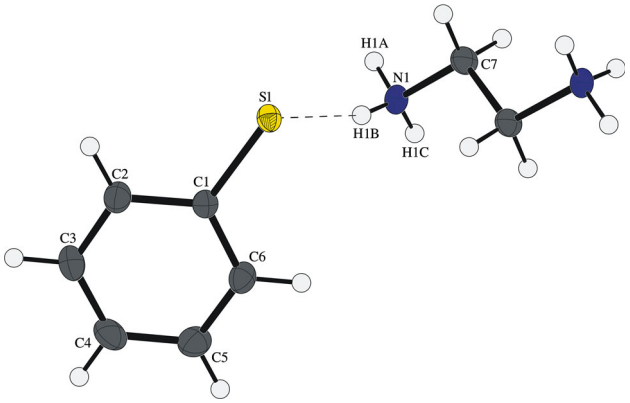

Fig. 1 Molecular structure of **1**, with the labeling scheme for the asymmetric unit and hydrogen bond interactions (shown as *dashed lines*). The diamine lies on twofold axis, so only half of the molecule is symmetrically independent. Displacement ellipsoids are drawn at the 50 % probability level (Color figure online)

with the Specac Quest single-reflection diamond attenuated total reflectance (ATR) accessory. Spectral analysis was controlled by the OMNIC software package. Melting points of new compounds were determined on SMP3 apparatus (Stuart Scientific, UK) and are uncorrected.

Preparation of 1,2-etanediammonium dithiophenolate 1

$C_6H_5S^{(-)(+)}NH_3(CH_2)_2H_3N^{(+)(-)}SC_6H_5$ ***1***

A solution of the C_6H_5SH (0.33 g, 3 mmol) was added dropwise to a solution of 1,2-etanediamine (0.06 g, 1 mmol) in propanol-2 (10 mL). The solvent was then added gradually until a white deposit formed was completely dissolved. The solution was left to stand at room temperature for a few days for crystallization. The obtained colorless crystals were suitable for X-ray diffraction analysis. Elemental analysis: Calc. for $C_7H_{10}NS$ (MW 140.22) C, 59.96; H, 7.19; N, 9.98; S, 22.87 %. Found: C, 59.82; H, 7.21; N, 10.02; S, 22.90 %. Mp 103–105 °C. FTIR (crystalline product) 3293 (s), 3211 (m), 3056 (s), 2925 (vs), 2807 (vs), 2725 (vs), 2580 (vs), 2156 (m), 2034 (s), 1616 (m), 1577 (s), 1521 (m), 1471 (s), 1456 (m), 1432 (m), 1359 (m), 1311 (w), 1255 (w), 1170 (m), 1114 (m), 1083

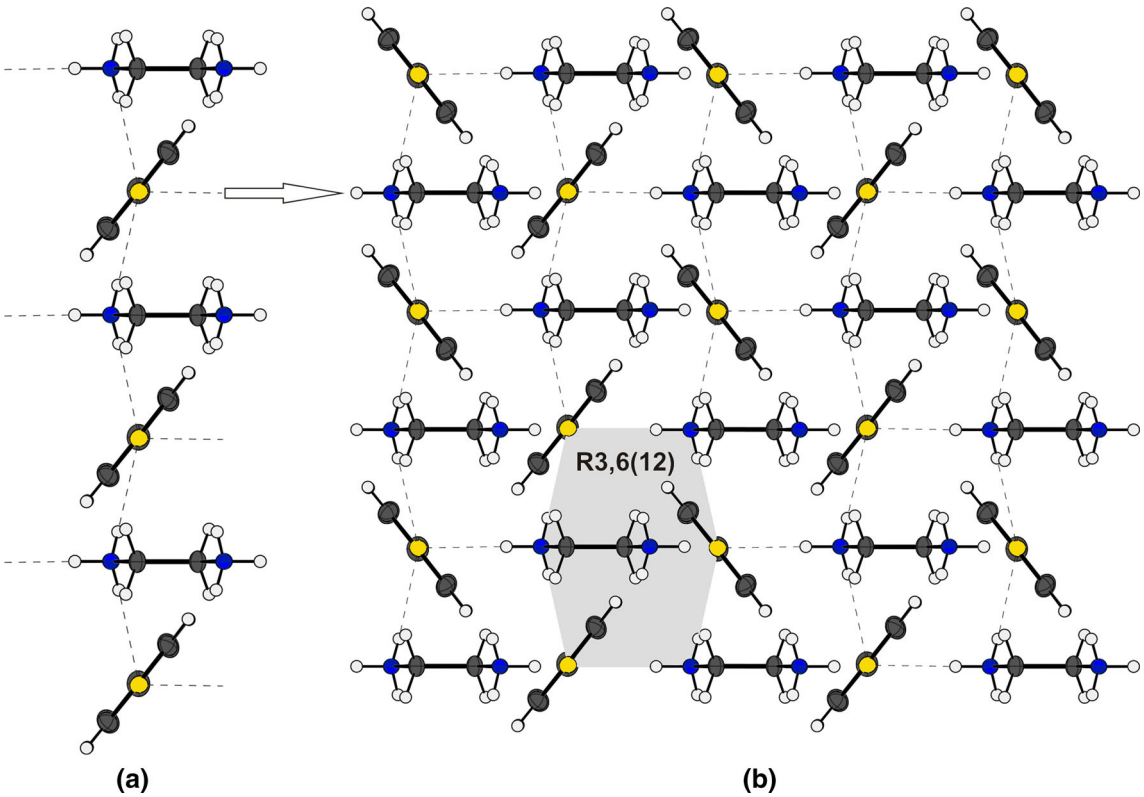

Fig. 2 Chain **a** of molecules of **1** and layer **b** linked by hydrogen bonds (Color figure online)

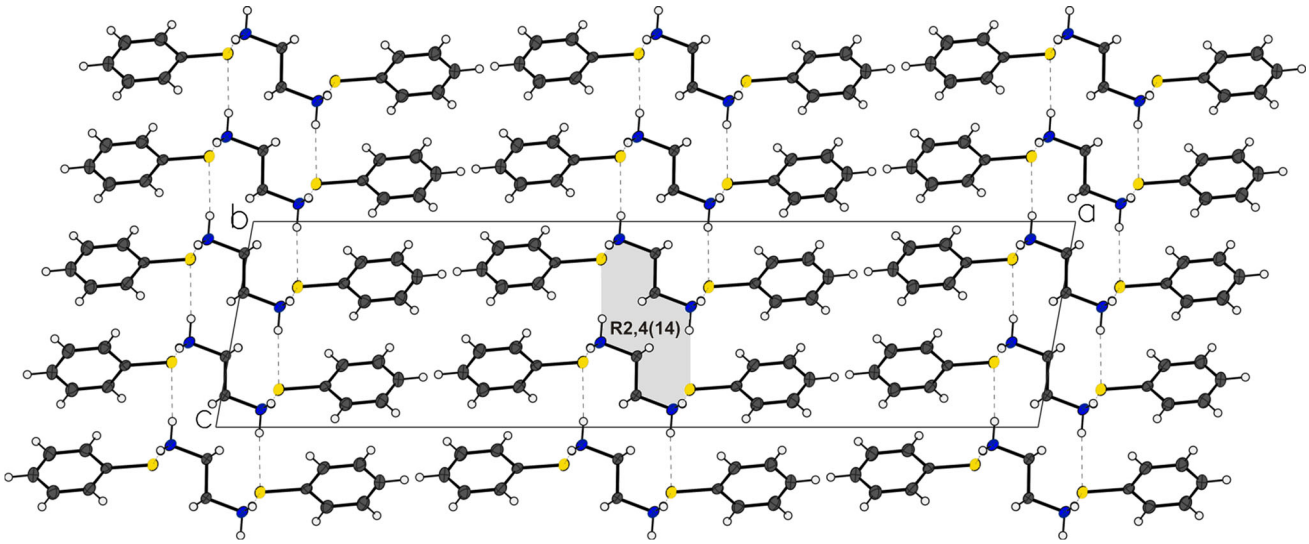

Fig. 3 Packing diagram for **1**. View direction is parallel to the crystallographic *b* axis (Color figure online)

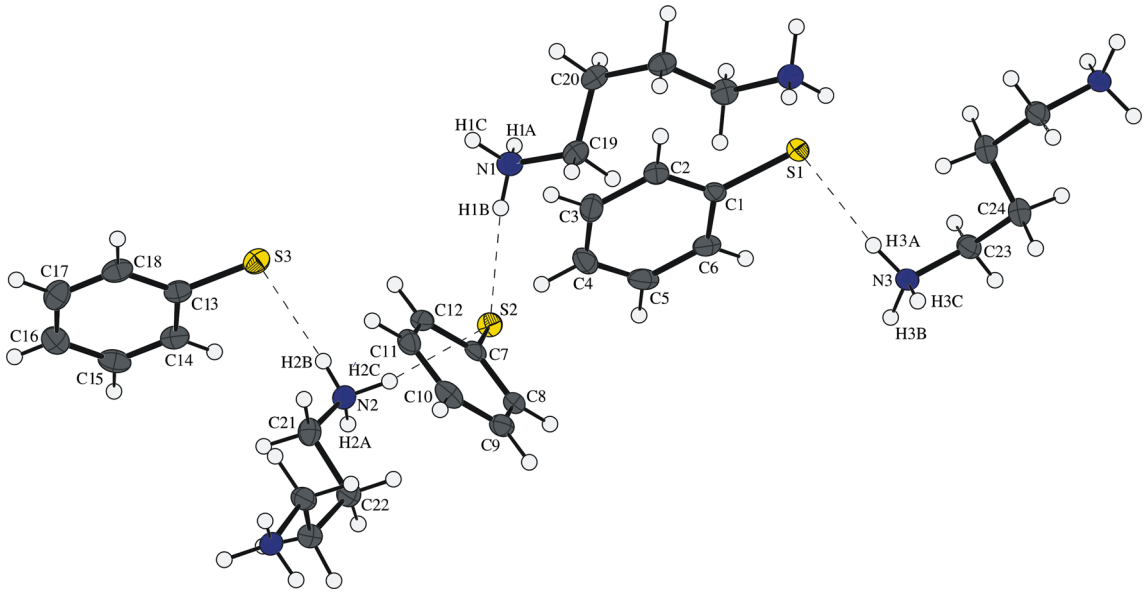

Fig. 4 Molecular structure of **2**, with the labeling scheme for the asymmetric unit and hydrogen bond interactions (shown as *dashed lines*). The diamines lie across a crystallographic twofold axis so that the asymmetric unit contains half of each molecule. Displacement ellipsoids are drawn at the 50 % probability level (Color figure online)

(s), 1047 (m), 1025 (m), 991 (s), 950 (vs), 825 (w), 821 (m), 740 (s), 696 (s), 568 (m) cm^{-1}.

Preparation of 1,4-butanediammonium dithiophenolate 2

$C_6H_5S^{(-)(+)}NH_3(CH_2)_4H_3N^{(+)(-)}SC_6H_5$ 2

1,4-butanediamine (0.09 g, 1 mmol) was dissolved in propanol-2 (10 mL) and was added to C_6H_5SH (0.66 g, 6 mmol). After standing for 1 week at room temperature, crystals of **2** formed and were suitable for X-ray analysis. Elemental analysis: Calc. for $C_{16}H_{24}N_2S_2$ (MW 308.49) C, 62.29; H, 7.84; N, 9.08; S, 20.79 %. Found: C, 62.19; H, 7.88; N, 9.11; S, 20.82 %. Mp 99–101 °C. FTIR (crystalline product) 3243 (m), 3115 (m), 3056 (s), 2844 (s), 2764 (s), 2692 (s), 2486 (s), 2073 (s), 1635 (w), 1572 (s), 1506 (m), 1464 (s), 1431 (s), 1385 (m), 1322 (m), 1079 (s), 1023 (s), 994 (m), 931(m), 887 (m), 844 (m), 820 (m), 733 (vs), 688(vs) cm^{-1}.

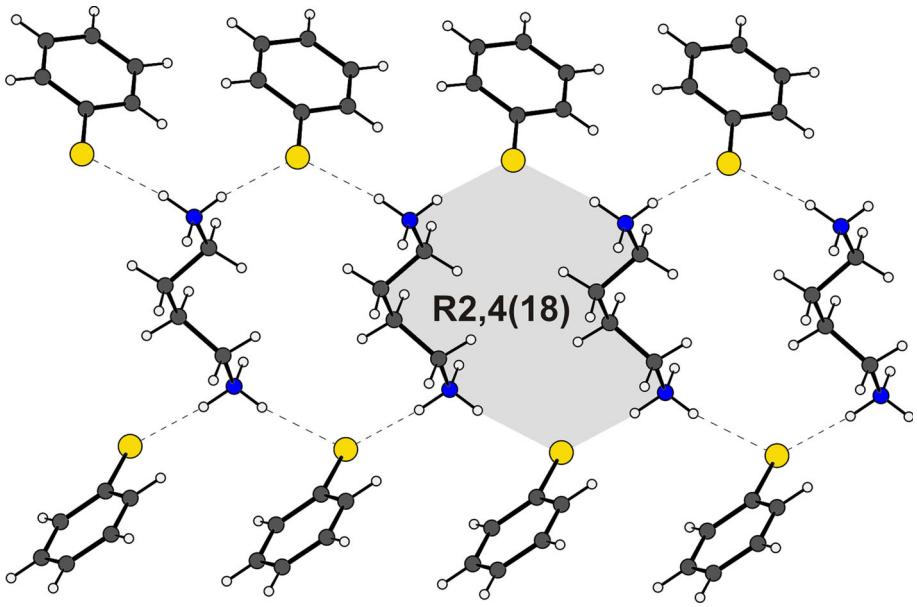

Fig. 5 Part of the crystal structure of **2**, showing the formation of a hydrogen-bonded ribbon built from $R_4^2(18)$ rings (Color figure online)

Preparation of 1,6-hexanediammonium dithiophenolate 3

$C_6H_5S^{(-)(+)}NH_3(CH_2)_6H_3N^{(+)(-)}SC_6H_5$ ***3***

To a solution of 1,6-hexanediamine (0,12 g, 1 mmol) in toluene (15 mL), thiophenol (0.33 g, 3 mmol) was added. Immediately, a white precipitate formed and this was dissolved by the addition of a portion of the solvent. The mixture was kept at 277 K for a few days, and colorless crystals of **3** suitable for X-ray diffraction were obtained. Elemental analysis: Calc. for $C_{18}H_{28}N_2S_2$ (MW 336.54) C, 64.24; H, 8.38; N, 8.32; S, 19.05 %. Found: C, 64.15; H, 8.41; N, 8.35; S, 19.12 %. Mp 116–118 °C. FTIR (crystalline product) 3335 (m), 3311 (m), 3269 (m), 3147 (m), 3054 (m), 2929 (vs), 2853 (vs), 2758 (s), 2552 (s), 2147 (m), 1633 (m), 1576 (s), 1557 (s), 1470 (s), 1456 (s), 1393 (s), 1319 (m), 1083 (m), 1064 (m), 997 (m), 943 (m), 749 (m), 728 (s), 696(s) cm^{-1}.

X-ray crystallographic study

Diffraction data were recorded on a KUMA KM4 diffractometer with graphite-monochromated Mo K_α radiation using sapphire-2 CCD detector (Oxford Diffraction Ltd). The apparatus was equipped with an open flow thermostat (Oxford Cryosystems) which enabled experiments at 150 K **1** and 120 K (other compounds). The stream of nitrogen also prevented the specimen from contact with moist and oxygen. The structures were solved by direct methods and refined using the program packages WinGX 2013.3 [33] and SHELX—2013 [34]. Because of low absorption of X-rays by the crystals, no absorption corrections were applied. All non-hydrogen atoms were refined anisotropically. Hydrogen atoms were refined in geometrically idealized position with isotropic temperature factors 1.2 times the equivalent isotropic temperature factors U_{eq} of their attached atoms (1.5 for CH_3 groups). Hydrogen atoms of ammonium groups were found in the electron density Fourier map and refined without constraints. The 1,4-butanediammonium molecule in **2** contained atom C24, which was refined as disordered over two positions (*s.o.f.* 0.699(15)/0.301(15)). The crystallographic data and some details of the structural refinement are summarized in Table 1. Structural details of hydrogen bonding are collected in Table 2.

Results and discussion

We decided to use 1,2-etanediamine, 1,4-butanediamine and 1,6-hexanediamine to study the influence the length of the carbon chain in aliphatic diamines on the pattern of the hydrogen bond network. The reaction of thiophenol with the diamines yields transparent crystal of: 1,2-etanediammonium thiophenolate **1**, 1,4-butanediammonium thiophenolate **2** and 1,6-hexanediammonium thiophenolate **3**. All salts reported here were formed with the thiophenol:amine ratio 2:1. Salts **1** and **2** were crystallized from propanol-2, **3** from toluene. The structures of three ammonium salts were determined by single-crystal X-ray diffraction.

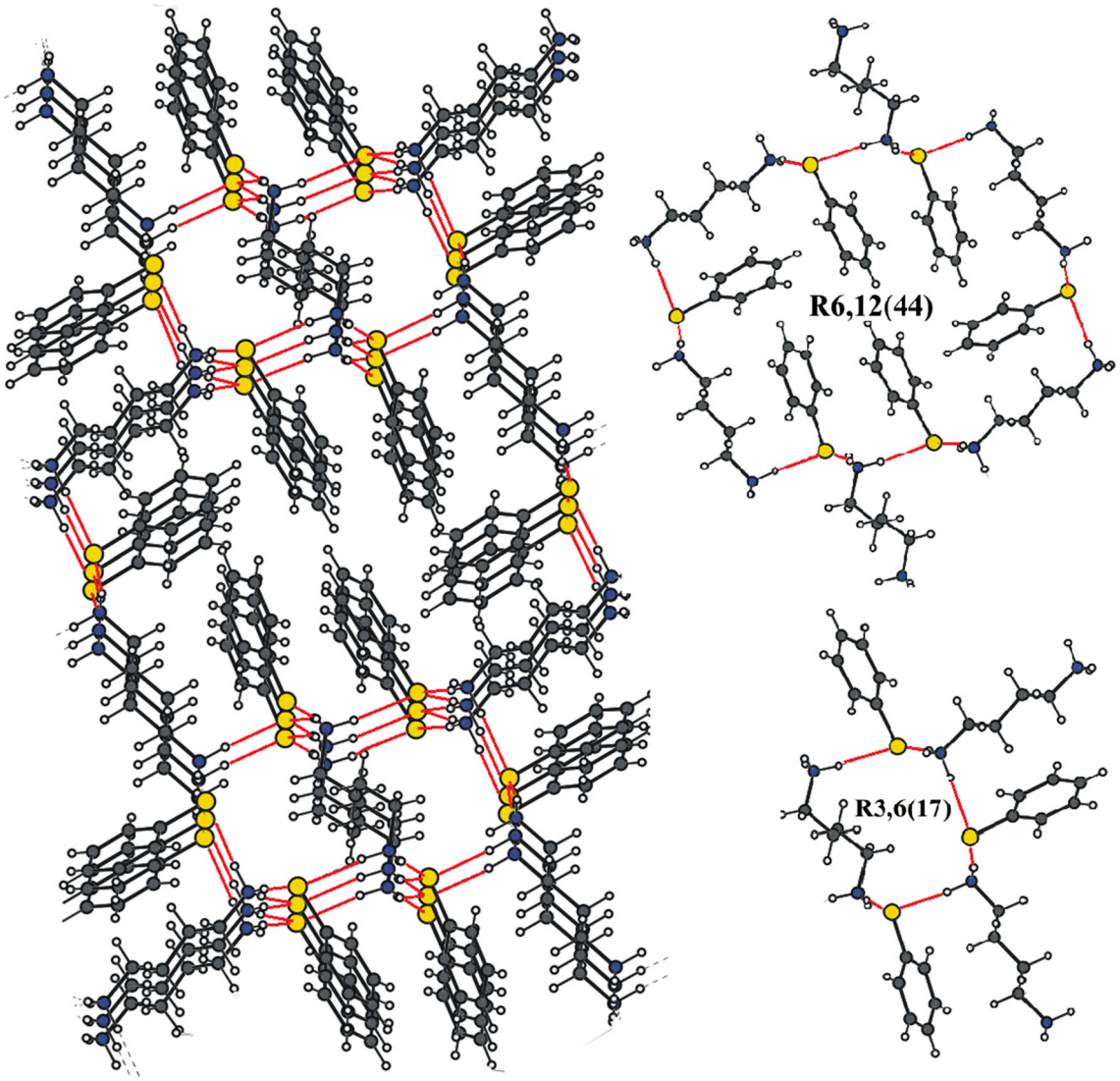

Fig. 6 A view of the 3-D supramolecular network of crystal **2**, showing hydrogen bonds as *red lines* (Color figure online)

Crystal structures of $C_6H_5S^{(-)(+)}NH_3(CH_2)_2H_3N^{(+)(-)}SC_6H_5$ 1

The independent unit of crystal of 1,2-etanediammonium thiophenolate **1** contains half 1,2-ethanediammonium cation and one thiophenolate anion (Fig. 1), which form cation···anion pairs through the hydrogen bonding interactions.

The illustration of crystal packing of **1** (Figs. 2, 3) brings more information about the studied system. It shows that two atoms of hydrogen from each of protonated amine groups form intermolecular NH···S hydrogen bonds with two adjacent thiophenolate anions, thus generating chain (Fig. 2a). The third atom of hydrogen from the same amino group is bonded to the sulfur atom from a parallel chain shifted relative to the first one by ½ of identity period of the chains (Fig. 2b). The rings of $C_6H_5S^{(-)}$ anions from the adjacent chains are twisted about angle 76.69°.

All six ammonium H atoms are involved in the formation of hydrogen bonds with six thiophenolate anions, and each anion accepts hydrogen bonds from three cations. Propagation of these hydrogen bonds generates two-dimensional (2-D) layer parallel to the (100), built of the larger rings described by the graph set $R_6^3(12)$ (Fig. 2b) and $R_4^2(14)$ (Fig. 3) [35, 36]. The diprotonated amine is sandwiched among the mercapto groups (Fig. 3). In addition, the packing of **1** is stabilized by relatively weak CH···π interaction (Table 2) between the thiophene rings from adjacent chains. No π–π stacking interactions can be found between neighboring aromatic rings in the crystal packing structures of **1**.

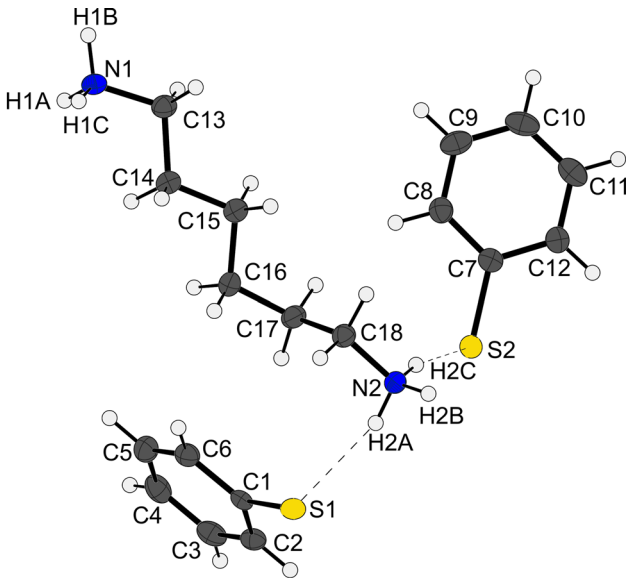

Fig. 7 Asymmetric unit of crystals **3**, with the labeling scheme and hydrogen bond interactions (shown as *dashed lines*). Displacement ellipsoids are drawn at the 50 % probability level (Color figure online)

Crystal structures of $C_6H_5S^{(-)(+)}NH_3(CH_2)_4H_3N^{(+)(-)}SC_6H_5$ 2

As can be seen in Fig. 4, the asymmetric unit of crystal 1,4-butanediammonium thiophenolate **2** consists of one and a half of ammonium cation and three thiophenolate anions.

In crystals of **2**, ions are connected with each other through the intermolecular NH···S hydrogen bonding to form 1-D ribbons made up of centrosymmetric $R_4^2(18)$ rings (Fig. 5).

Three adjacent ribbons are further linked by hydrogen bonding interactions between anionic sulfur atoms and hydrogen linked to positively charged nitrogen atoms, to form a 3-D supramolecular network. In this way, two types of rings with the graph sets $R_6^3(17)$ and $R_{12}^6(44)$ are generated (Fig. 6). There are also relatively weak CH···π interactions (Table 2) present in **2**, and these involve both the amine and the thiophenol.

Fig. 9 Crystal packing of **3**. A view of the 2-D layers (*red*) and 3-D▶ supramolecular network (*blue*) (**a**) and layer linked by hydrogen bonds forming centrosymmetric dimer (**b**). Hydrogen bonds are denoted as *red lines* (Color figure online)

Crystal structures of $C_6H_5S^{(-)(+)}NH_3(CH_2)_6H_3N^{(+)(-)}SC_6H_5$ 3

The structure of crystal 1,6-hexanediammonium thiophenolate **3** consists of one diammonium cation and two thiophenolate anions (Fig. 7).

Similar to crystals of **2**, in **3** all the components in the unit cell are connected via $N^{(+)}$–H···$S^{(-)}$ hydrogen bonds to generate 1-D ribbons, built of $R_4^2(22)$ rings (Fig. 8).

In comparison with the crystals **2** to **3**, ribbons are arranged 2-D layer (Fig. 9a) parallel to the (001).

These layers are further linked by $N^{(+)}$–H···$S^{(-)}$ hydrogen bonds involving the other protonated amine groups and thiophenolate anions forming centrosymmetric dimers with the graph sets motif $R_4^2(8)$ (Fig. 9b). Our earlier studies have shown that such eight-membered rings with four donors and two acceptors were characteristic for other ammonium salts [26, 27, 37, 38]. The final result of the interactions is infinite 3-D supramolecular network (Fig. 9a) strengthened by C–H···π interactions (Table 2) different from the 3-D network of crystal **2**.

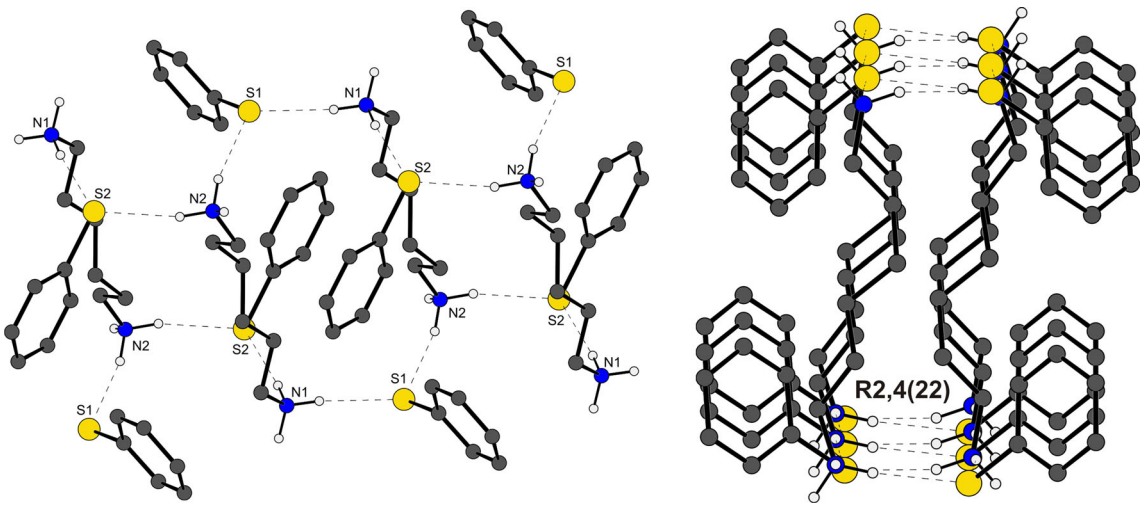

Fig. 8 Part of the crystal structure of **3**, showing the formation of a hydrogen-bonded ribbons built from $R_4^2(22)$ rings (Color figure online)

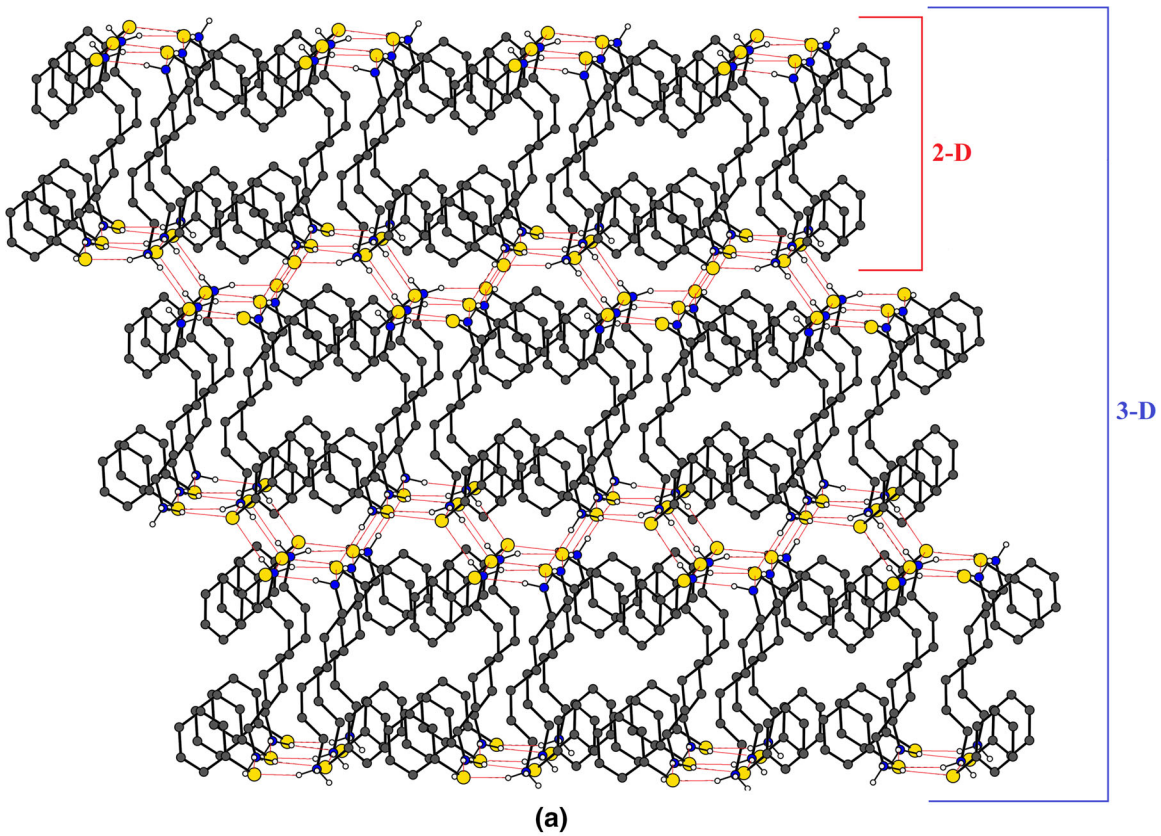

(a)

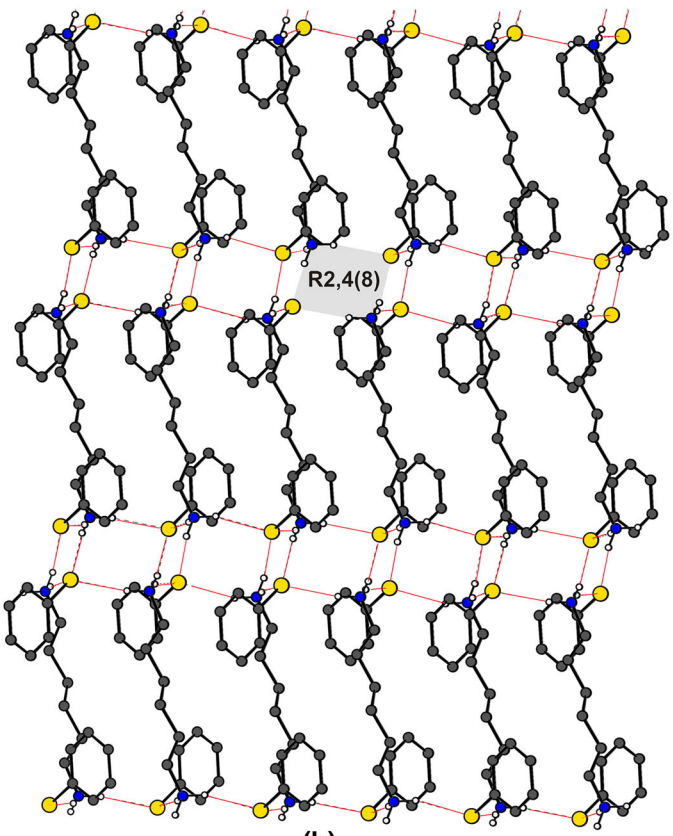

(b)

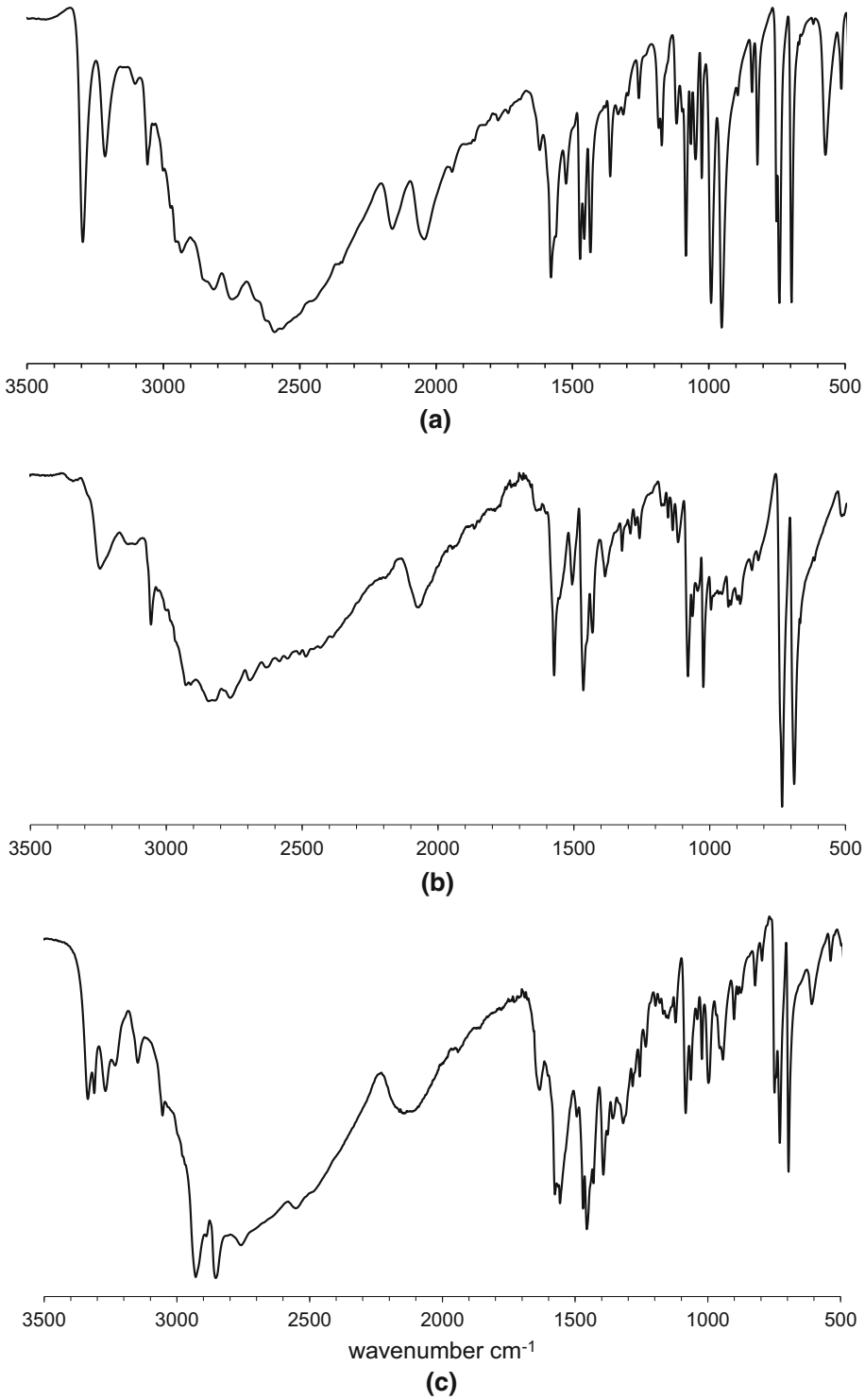

Fig. 10 FTIR spectra crystalline product of **1** (**a**), **2** (**b**) and **3** (**c**)

The N···S distances in three salts lie in the range 3.155 (3)–3.286 (3) Å, comparable with values observed in other silanethiolates [26, 27], aromatic thiolate [25, 39, 40], ditiocarbamates [41–43] or sulfides [44–46].

Structural analyses indicate that the aromatic rings of the $C_6H_5S^{(-)}$ anions and methylene groups of diammonium in all crystals are involved in the C–H···π interactions [47], whereas π···π interactions among these aromatic rings are

not observed. Full details of the hydrogen bond geometries are given in Table 2.

Spectral characterization

The infrared range 4000–700 cm^{-1} is most commonly used in the study of formation hydrogen bonds. Changes are the strongest in the vibrational bands of the proton-donor groups and weaker in the vibrational bands of the proton-acceptor groups. These changes have an impact on the intensity, position, width and shape of the contour bands of oscillating spectra. Interesting results in IR spectroscopy for the measurement of hydrogen bridges are achieved for molecules packed in the crystal lattice. Properties of molecules in a crystal lattice differ from properties of the same molecule in gaseous or liquid phase.

The IR spectra for the three studied crystalline substances are very similar (Fig. 10). The stretching bands in the range 3350–3150 cm^{-1} can be attributed to the vibration of the primary ammonium cations [46]. The spectrum of the zwitterionic amino acid L-tyrosine shows the effect of protonation of the amino group, with the N–H stretching vibration occurring over a broad range 3100–2600 cm^{-1} [48]. In the spectrum, we can see the very broad and strong stretching bands appearing in the range of 3000–2200 cm^{-1} that are characteristic in the case of the formation of extensive hydrogen bonding interactions [49]. The continua overlap with stretching vibration of aromatic C–H at 3100–3000 cm^{-1} and C–H stretching present in diamines molecules at 3000–2850 cm^{-1}, as well as the very weak stretching bands of the S–H bonds usually registered 2600–2550 cm^{-1} [50, 51]. Primary aliphatic amines can be additionally confirmed by the characteristic bands at 1600–1570 which correspond to bending (deformation) vibration NH_3^+ [25] and C–N stretching vibration located at 1250–1020 cm^{-1}. N–H out-of-plane bending (wagging) absorptions for aliphatic amines are found at 660–910 cm^{-1} [52]. The bands appearing in the range of 1500–1400 cm^{-1} are attributed to the C = C stretching vibrations of the aromatic rings.

Conclusion

In this work, it was demonstrated that in all three compounds, proton transfer has occurred, between –SH and NH_2 groups leading to $^{(+)}$N–H···S$^{(-)}$ hydrogen bonding interactions. It seems that the proton transfer and formation of charge-assisted NH···S hydrogen bonds is controlled not only by the acidity and basicity of the partners but also by the possibility of formation of a net of hydrogen bonds. Structural analyses indicate that increasing the length of alkyl chain in aliphatic diamines can influence the pattern of the hydrogen bonding network. The structures of compounds **1**–**3** are all different, and each exploits significant numbers of non-covalent bonding of H bonds and C–H···π interactions, which play crucial roles in the formation of supramolecular networks. None of the studied crystals featured π···π stacking interactions. The crystallographic investigation revealed that elongation of the spacer between the ammonium groups caused the conversion of a two-dimensional (2-D) layer found in the crystal of **1** into three-dimensional (3-D) supramolecular network present in crystals of **2** and **3**. The transfer of proton from the thiol to the diamines was confirmed by the FTIR. The spectra of crystalline diammonium thiophenolates shows the effect of protonation of the amino group, with the strong N–H stretching vibration occurring over a very broad range 3300–2600 cm^{-1}.

Supplementary data

CCDC Nos. 1430358–1430360 (for compounds **1**, **2** and **3**, respectively) contain the supplementary crystallographic data for this paper. These data can be obtained free of charge on request, quoting the deposition number, at www.ccdc.cam.ac.uk/conts/retrieving.html [or from the Cambridge Crystallographic Data Centre, 12 Union Road, Cambridge CB2 1EZ, UK; fax: (international) +44-1223/336-033; E-mail: deposit@ccdc.cam.ac.uk].

Acknowledgments Author thanks Dr Anna Dołęga and Dr Jarosław Chojnacki for helpful discussion during preparation of the manuscript.

References

1. Desiraju GR (2003) J Mol Struct 656:5
2. Desiraju GR (2010) J Chem Sci 122:667
3. Politzer P, Murray JS, Clark T (2013) Phys Chem Chem Phys 15:11178
4. Politzer P, Murray JS, Clark T (2015) Top Curr Chem 358:19
5. Steiner T (2002) Angew Chem Int Ed 41:48
6. Desiraju GR (2001) Nature 412:397
7. Parthasarathi R, Subramanian V, Sathyamurthy N (2006) J Phys Chem A 110:3349
8. Jeeffrey GA (1997) An introduction to hydrogen bonding. Oxford University Press, Oxford
9. Aakeröy CB, Beatty AM (2001) Aust J Chem 54:409

10. Desiraju GR, Steiner T (1999) The weak hydrogen bond in structural chemistry and biology. Oxford University Press, Oxford
11. Allen FH (2002) Acta Crystallogr Sect B 58:380
12. Yutronic N, Manriquez V, Jara P, Wittke O, Gonzalez G (2001) Supramol Chem 12:397
13. Shibahara F, Kobayashi S, Maruyama T, Murai T (2013) Chem Eur J 19:304
14. Nather C, Jess I, Jones PG, Taouss C, Teschmit N (2013) Cryst Growth Des 13:1676
15. Kuan FS, Mohr F, Tadbuppa PP, Tiekink ERT (2007) Cryst Eng Comm 9:574
16. Kubota NK, Iwamoto H, Fukazawa Y, Uchio Y (2005) Heterocycles 65:2675
17. Batsanov AS, Fox MA, Hibbert TG, Howard JAK, Kivekas R, Laromaine A, Sillanpaa R, Vinas C, Wade K (2004) Dalton Trans 2004:3822
18. Hanif M, Qadeer G, Rama NH, Vuoti S, Autio J (2007) Acta Crystallogr Sect E 63:o4507
19. Ambalavanan P, Palani K, Ponnuswamy MN, Thirumuruhan RA, Yathirajan HS, Prabhuswamy B, Raju CR, Nagaraja P, Mohana KN (2003) Mol Cryst Liq Cryst 393:67
20. Holynska M, Kubiak M (2009) Acta Crystallogr Sect C 65:o191
21. Miyamae H, Oikawa T (1985) Acta Crystallogr Sect C 41:1489
22. Gerner R, Kiel G, Gattow G (1985) Z Anorg Allg Chem 523:76
23. Kilian P, Pazdera P, Marek J, Novosad J, Touzin J (1998) Z Anorg Allg Chem 624:1497
24. Crawford MJ, Klapotke TM, Mayer P, Vogt M (2004) Inorg Chem 43:1370
25. Jetti RKR, Boese R, Thakur TS, Vangala VR, Desiraju GR (2004) Chem Commun 2004:2526
26. Becker B, Baranowska K, Chojnacki J, Wojnowski W (2004) Chem Commun 2004:620
27. Baranowska K, Chojnacki J, Konitz A, Wojnowski W, Becker B (2006) Polyhedron 25:1555
28. Baranowska K, Roman P, Socha J (2009) Acta Crystallogr Sect E 65:o282
29. Baranowska K, Piwowarska N (2008) Acta Crystallogr Sect E 64:o178
30. Baranowska K (2007) Acta Crystallogr Sect E 63:o2653
31. Baranowska K, Chojnacki J, Wojnowski W, Becker B (2003) Acta Crystallogr Sect E 59:o2022
32. Baranowska K, Piwowarska N, Herman A, Dołęga A (2012) New J Chem 36:1574
33. Farrugia LJ (2012) J Appl Crystallogr 45:849
34. Sheldrick GM (2008) Acta Crystallogr Sect A 64:112
35. Bernstein J, Davis RE, Shimoni L, Chang NL (1995) Angew Chem Int Ed Engl 34:1555
36. Etter MC (1990) Acc Chem Res 23:120
37. Baranowska K, Chojnacki J, Gosiewska M, Wojnowski W (2006) Z Anorg Allg Chem 632:1086
38. Baranowska K, Liadis K, Wojnowski W (2008) Acta Crystallogr Sect E 64:o1329
39. Baranowska K, Chojnacki J, Becker B, Wojnowski W (2003) Acta Crystallogr Sect E 59:o765
40. Chadwick S, Englich U, Noll B, Ruhlandt-Senge K (1998) Inorg Chem 37:4718
41. Mietlare-Kropidłowska A, Chojnacki J, Wityk P, Wieczór M, Becker B (2012) Acta Crystallogr Sect E 68:o1717
42. Wahlberg A (1978) Acta Crystallogr Sect B 34:3822
43. Teske CL, Bensch W (2010) Z Anorg Allg Chem 636:356
44. Shishkin OV, Kolos NN, Orlov VD, Kuznetsov VP, Lakin EE (1995) Acta Crystallogr Sect C 51:2643
45. Andras MT, Hepp AF, Fanwick PE, Martuch RA, Duraj SA, Gordon EM (1996) Acta Crystallogr Sect C 52:1701
46. Bottcher P, Buchkremer-Hermanns H, Baron J (1984) Z Naturforsch Teil B Chem Sci 39:416
47. Deng ZP, Huo LH, Zhao H, Gao S (2012) Cryst Growth Des 12:3342
48. Anderson RJ, Bendell DJ, Groundwater PW (2004) Organic spectroscopic analysis University of Sunderland. The Royal Society of Chemistry, London
49. Zundel G, Brzeziński B (1998) Pol J Chem 72:172
50. Barth A (2000) Prog Biophys Mol Biol 74:141
51. Marynowski W, Klucznik T, Baranowska K, Dołęga A, Wojnowski W (2010) Z Anorg Allg Chem 636:685
52. Nakamoto K (1997) Infrared and Raman spectra of inorganic and coordination compounds, 5th edn. Wiley, Hoboken